CIRRELT

Centre interuniversitaire de recherche
sur les réseaux d'entreprise, la logistique et le transport

Interuniversity Research Centre
on Enterprise Networks, Logistics and Transportation

Closed-Loop Supply Chain Network Design under Uncertain Quality Status: Case of Durable Products

Mohammad Jeihoonian
Masoumeh Kazemi Zanjani
Michel Gendreau

November 2015

CIRRELT-2015-56

Bureaux de Montréal :
Université de Montréal
Pavillon André-Aisenstadt
C.P. 6128, succursale Centre-ville
Montréal (Québec)
Canada H3C 3J7
Téléphone : 514 343-7575
Télécopie : 514 343-7121

Bureaux de Québec :
Université Laval
Pavillon Palasis-Prince
2325, de la Terrasse, bureau 2642
Québec (Québec)
Canada G1V 0A6
Téléphone : 418 656-2073
Télécopie : 418 656-2624

www.cirrelt.ca

Closed-Loop Supply Chain Network Design under Uncertain Quality Status: Case of Durable Products

Mohammad Jeihoonian[1,2,*], Masoumeh Kazemi Zanjani[1,2] , Michel Gendreau[1,3]

[1] Interuniversity Research Centre on Enterprise Networks, Logistics and Transportation (CIRRELT)

[2] Department of Mechanical and Industrial Engineering, Concordia University, 1515, St-Catherine, St. West, EV4.139, Montréal, Canada H3G 1M8

[3] Department of Mathematics and Industrial Engineering, Polytechnique Montréal, P.O. Box 6079, Station Centre-ville, Montréal, Canada H3C 3A7

Abstract. This paper proposes a two-stage stochastic mixed-integer programming model for a closed-loop supply chain network design problem in the context of modular structured products in which the reverse network involves several types of recovery options. It accounts for uncertainty in the quality status of the return stream, modeled as binary scenarios for each component in the reverse bill of material corresponding to such products. To deal with the intractable number of scenarios in the proposed model, a scenario reduction scheme is adapted to the problem of interest to preserve the most pertinent scenarios based on a modified Euclidean distance measure. The reduced stochastic large-scale optimization problem is then solved via a L-shaped algorithm enhanced with surrogate constraints and Pareto-optimal cuts. Numerical results indicate that the scenario reduction algorithm provides good quality solutions to the stochastic problem in a reasonable amount of time through applying the enhanced L-shaped method.

Keywords. Stochastic closed-loop supply chain, uncertain quality status, durable products, scenario reduction, L-shaped.

Acknowledgment. The authors would like to thank the Fonds de recherche du Québec - Nature et technologie (FRQNT), for the financial support in this research project.

* Corresponding author: Mohammad.Jeihoonian@cirrelt.ca

Dépôt légal – Bibliothèque et Archives nationales du Québec
Bibliothèque et Archives Canada, 2015

1. Introduction

In response to sustainability of supply chains, design and management of closed-loop supply chains (CLSC) have attracted a growing interest over the recent decade. It has been recognized that CLSCs comprise forward channel along with the so-called "reverse supply chain (RSC)". The focus of RSC is on taking back of end-of-life and end-of-use products (cores) from consumers, and recovering added value by reusing the entire product, and/or some of its components, such as modules and parts [1]. The prime importance of CLSCs is attributed to the environmental footprint of cores as well as the profitability of recovery practices. Needless to say, the prosperity of such business practices requires placing appropriate reverse logistics infrastructures and managing arising return flows efficiently. Therefore, the design of the CLSC is becoming increasingly important.

CLSC network design refers to decisions for locating several types of facilities in both forward and reverse chains in addition to efficiently routing and coordinating physical forward and reverse flows. Designing a CLSC network for durable products, that are characterized by their modular structured design and their long life cycle (e.g., computers and large household appliances), is a complex problem. Such category of products can be disassembled into several components (i.e., modules and parts) as well as raw materials concerning the reverse bill of materials (BOM). Consequently, the reverse supply chain of such products involves various types of recovery facilities associated with different components in the reverse BOM of durable products. We note that in the context of CLSC/RSC network design, most studies are limited to involving a few recovery activities, e.g., remanufacturing and material recycling, in designing their networks. To fill the void in such a line of research, we, however, incorporate various recovery options, which an OEM can adopt in tackling the return stream. These recovery processes are plausible in taking different sub-assemblies of a typical durable product.

It is a well-known fact that a high level of uncertainty is a characteristic for various product recovery systems [2]. A clear distinction that is made between CLSCs and the traditional forward supply chains lies in uncertain condition (quality) of cores. This issue also add to the complexity of CLSC design for case of used durable products. In contrast, the existing stream of literature explicitly lacks accounting such unavoidable aspect in CLSC/RSC network design. That is, in the modeling framework, some simplifying assumptions have been made with respect to the quality variation of the return flows, thereby alleviating the complexity of the proposed model. More precisely, the concerned literature has focused on classifying cores with respect to deterministic disjoint quality levels [3–5], which ignores the uncertainty. Another attempt to model uncertain quality has been considering the rate of recovery as a random variable [6]. Nonetheless, both of the above-mentioned approaches are rough approximations of the uncertain quality status of cores.

Observing this major drawback, in this study, as our prime contribution, we propose a more precise approach to model the uncertain quality status, where the availability of each component in the reverse BOM is modeled as a discrete scenario following a Bernoulli distribution. This novel approach leads to an explicit incorporation of the uncertain quality status of returns. In this regard, we formulate this large-scale optimization problem as a two-stage stochastic mixed-integer program with recourse [7]. As far as the authors are aware, design of a CLSC concerning the explicit modeling of the uncertain quality of each component in the reverse BOM has never been investigated in the context of durable products.

On account of the fact that proposing the aforementioned approach for modeling the uncertain quality exponentially increases the number of scenarios, as the second contribution, we implement fast forward selection algorithm [8, 9] adapted to our problem setting as a scenario reduction technique to keep the most pertinent scenarios. Further, on the methodological side, our third contribution is to develop an enhanced solution approach based on L-shaped method [10], which shows a consistent performance efficiency in our experimentations. The classical L-shaped scheme results from applying Benders decomposition [11] to two-stage stochastic programming models with continuous variables. This decomposition approach typically requires algorithmic refinements to accelerate its convergence. We, therefore, provide enhancement strategies that include adding induced constraints to the master problem to restrict its feasible region and also generating Pareto-optimal cuts to strengthen the deepness of optimality cuts throughout the execution of the solution algorithm. Even though it is beyond the scope of this paper, it should be stated that the uncertain demand of brand-new products as well as quantity of returns can also be taken into account as other sources of uncertainty in designing the CLSC network.

The remainder of this paper is organized as follows. In the next section, we provide the review of the relevant literature. In Section 3, we introduce the problem setting and its two-stage stochastic programming formulation. Section 4 elaborates on the scenario reduction algorithm. In Section 5, a detailed description of the enhanced L-shaped method is given. Section 6 presents computational experiments on the performance of the proposed solution method for a large household appliance example. In the last Section, we provide concluding remarks and future research directions.

2. Literature review

Many efforts have been made to model and optimize deterministic CLSC/RSC network design problems. The current literature in the context of product recovery offers a variety of problems spanning from recycling of simple waste, such as carpet and sand to different recovery options of more complex products [3–5, 12–17]. For an extensive review of proposed models and cases, the reader is referred to [18, 19].

The overview of the existing literature implies that in most of prevailing studies uncertainty consideration is limited to demand and quantity of returns. On the other hand, the impact of uncertain quality state of returns on CLSC design, regardless of its substantial impact, has not been adequately investigated in the literature. The most common approach that makes an explicit attempt to incorporate uncertainty in design parameters is stochastic optimization methods. Since the seminal work of Salema et al. [20], in which the authors addressed a CLSC network design problem under uncertain demand and quantity of returns, some researchers have developed two-stage stochastic programming formulations to model such stochastic parameters. Details of these studies can be found in [21–25]. The analysis of the current literature suggests the following observations: 1) most of them are case oriented logistical networks; 2) the number of scenarios is quite small (e.g., twelve scenarios in [21]); and, 3) concerning the size of test problems, the optimal solution is found by virtue of commercial softwares. It should be stated that [21] is an exception to the last observation such that an integer L-shaped algorithm was devised as the solution approach. Nonetheless, its algorithmic framework is only suited for addressing situations with a very small number of scenarios.

To the best of our knowledge the only work that captures uncertainty in the quality status of returns has been recently presented by Chen et al. [6], in which the rate of recovery is considered as a measure to reflect the quality status of cores. Accordingly, the authors modeled the random recovery rate as a set of scenarios for a CLSC network design, including collection and remanufacturing facilities in the reverse channel. The resulting two-stage stochastic quadratic formulation was solved via the integer L-shaped method integrated with the sample average approximation scheme. As highlighted in the preceding section, we, however, capture the uncertain quality status of the return stream in a more precise setting with regard to the reverse BOM in the context of modular structured products. Our approach differs in the scope from [6] in the sense that: 1) it discriminates the quality state of cores in terms of the availability of components in the reverse BOM of a durable product; 2) it involves various types of recovery options plausible for the sub-assemblies of a durable product; 3) the choice of the recovery process for each component depends on its quality status; and 4) the enhanced L-shaped method together with the proposed scenario reduction strategy is capable of serving as a viable tool for designing a realistic-scale CLSC network with quite crude information of quality status.

3. Problem description and formulation

In what follows, first, the description of the CLSC network applicable for durable products is presented. Then, we articulate how to model the random quality status of cores. Finally, we formulate the CLSC network design problem as a two-stage stochastic mixed-integer program with recourse.

3.1. CLSC network design for durable products

In the CLSC network design problem of interest, an organization operates a well-established forward channel in which the forward network comprises components and raw materials suppliers, manufacturing facilities, distribution centers, and end-user locations. The organization tends to adopt some suitable recovery practices to satisfy the directive recycling target stipulated by the legislator as well as to reclaim the economic value from used components. Hence, the aim is to extend the existing forward network to accommodate the recovery facilities and consequently to coordinate the physical forward and reverse flows in the extended supply chain network. The reverse network includes collection, disassembly, remanufacturing, bulk recycling, material recycling, and disposal centers, referred to as the recovery facilities. The returned durable products received at end-user sites are shipped to disassembly centers through collection centers. In our problem setting, the quality status of a returned durable product is defined as the availability of modules and parts for remanufacturing and part harvesting/reusing practices along with the mass of residues for bulk recycling processes. In disassembly centers, the inspected return stream is disassembled into different components based on the reverse BOM. The recoverable modules and recyclable materials are then sent to remanufacturing and recycling centers for further processes. Besides, the bulk of mixed residues would typically be processed in bulk recycling centers and/or outsourced to a third-party provider to separate the precious raw materials from mixed scrap, e.g., electronic scrap. The bulk recycling step is followed by material recycling and landfilling/incineration at disposal points. The material recycling step is designed to recover the raw materials after the execution of unit operations in bulk recycling sites. The non-valuable remaining, i.e., process waste, should be safely disposed of at disposal centers. The remanufactured modules, spare parts, and recycled raw materials are used for the following purposes: 1) shipping to manufacturing facilities to deploy in manufacturing of brand-new products; and, 2) selling on potential secondary markets. Given the above description, the conceptual structure of the CLSC under consideration is schematically illustrated in Figure 1. The solid arcs indicate the forward flows while the dashed ones denote the reverse flows in the CLSC.

3.2. Modeling random quality states of the return stream

The quality status of returns is indeed affected by the changes having been made during the lifetime of durable products. More specifically, in many cases, due to the usage and the deterioration rates during the long life cycle of such products, it is quite impossible to foresee the exact number of recoverable components in a returned durable product. Moreover, the quality status can only be revealed after grading the returned items in disassembly centers. In this study, the random quality state is considered as the availability of each component in the reverse BOM and modeled as discrete scenarios with Bernoulli probability distribution. Let P and L denote, re-

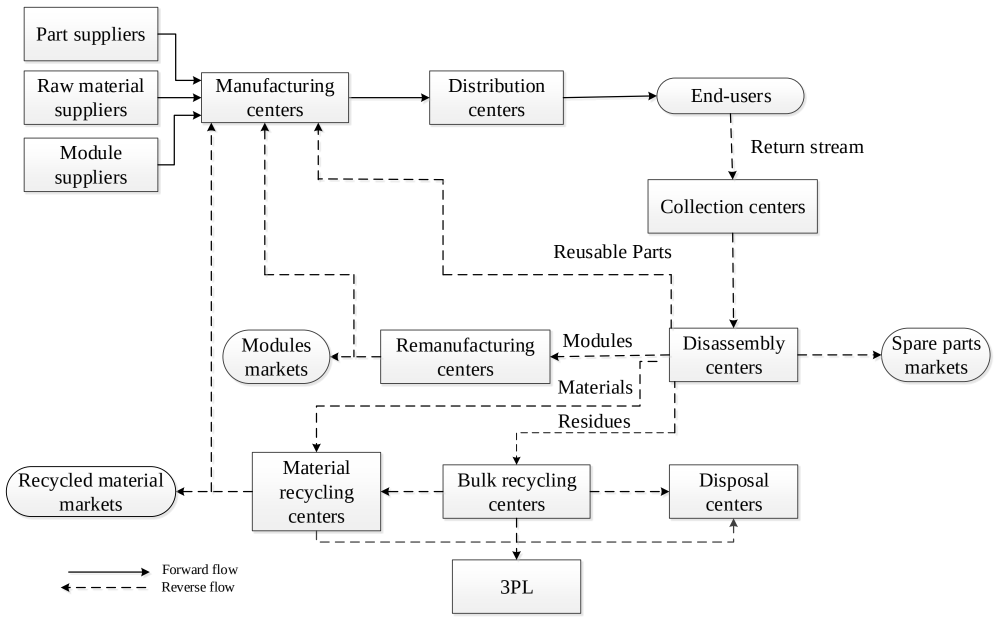

Figure 1: General structure of the CLSC network

spectively, the set of parts and modules in the brand-new durable product. Further, let γ_p, δ_l, and β denote, respectively, the number of reusable part p, the number of remanufacturable module l, and the mass of residues in the returned durable product. Now that we represent the random quality vector by $\boldsymbol{\xi}$ where $\boldsymbol{\xi} = \{\gamma_p|\forall\ p \in P; \delta_l|\forall\ l \in L; \beta\}$. We also represent each particular realization (scenario) of the random quality status by $\gamma_p(\boldsymbol{\xi}_s)$, $\delta_l(\boldsymbol{\xi}_s)$, and $\beta(\boldsymbol{\xi}_s)$. Each particular scenario s is associated with a non-negative probability π_s such that $\sum_{s \in S} \pi_s = 1$. Once the grading process is executed in disassembly centers, it is realized whether or not a particular part/module is suitable for the effective recovery process. We assume that the grading process yields a good condition component with success probability $\hat{p}$ otherwise a poor state one with a failure probability $\hat{q} = 1 - \hat{p}$. It should be emphasized that the success probability of each component (module/part) is the same in all returned items. Moreover, we assume that the probability distribution corresponding to the condition of different returned items are independent and identical.

For instance, we point out to a used twin tub of a washing machine such that each washing tube unit weighs 3.5 kg. Every unit can independently be either functional with probability $\hat{p}$ or defective with probability $\hat{q}$. Hence, the outcome of the grading process for the washing tube follows a Bernoulli distribution. Likewise, the quality status of other components in the reverse BOM is an independent random variable following a Bernoulli distribution. For every realization of the random quality vector, i.e., $\boldsymbol{\xi_s}$, we define an indicator function for each unit j of part p and another indicator function for each unit k of module l as follows.

$$I(p^j) = \begin{cases} 1 & \text{if unit } j \text{ is in a functional state;} \quad j = 1, ..., n^p \\ 0 & \text{otherwise} \end{cases}$$

$$I(l^k) = \begin{cases} 1 & \text{if unit } k \text{ is in a functional state;} \quad k = 1, ..., n^l \\ 0 & \text{otherwise} \end{cases}$$

It allows us to consider, respectively, the number of reusable part p as $\gamma_{ps} = \sum_{j=1}^{n^p} I(p^j)$ and the number of remanufacturable module l as $\delta_{ls} = \sum_{k=1}^{n^l} I(l^k)$. For example, in the aforementioned washing machine case, a possible outcome of the grading process might be one fully functional and one defective washing tube. Thus, for this specific part, γ is equal to 1. On the other hand, the indicator function of the defective unit takes 0 with probability $\hat{q}$. The defective unit will considered as residues and the viable recovery option for this unit will be bulk recycling process. In this regard, β will be increased with the corresponding weight of the unit, i.e., 3.5 kg and thus β is equal to 3.5 kg. In other words, all defective units observed after the grading operation are considered as residues and β is equal to the total summation of their corresponding weights.

The scenario generation approach described above results in 2^n scenarios for a typical durable product that consists of n different types of components. The probability of each scenario can be calculated as follows.

$$\pi_s = \hat{p}^{\gamma_{ps}+\delta_{ls}}.\hat{q}^{n^p+n^l-\gamma_{ps}-\delta_{ls}}$$

For example, suppose another washing machine that comprises ten different types of parts, namely P1, P2, ..., P10 and two different types of modules, namely L1 and L2 such that it involves only one unit per each type of parts and modules. Further, each component can be functional with probability 0.3, i.e., $\hat{p} = 0.3$. Consequently, the grading process results in 2^{12} scenarios. Table 1 presents five scenarios and their corresponding probability of occurrence among all possible realization of quality state scenarios for the grading process of this washing machine.

As shown in Table 1, in the first scenario (the first row of the table), there are six parts in functional condition and the others are considered as residues and should be treated in bulk recycling to recover their precious materials. Therefore, the value of the parameter γ is equal to 6. Likewise, only one module, i.e., L1, is remanufacturable and thus δ is equal to 1. The parameter β is then equal to the total weights of the components taking value of 0 in the first scenario, i.e., P2, P3, P7, P9, and L2. The probability of the first scenario is calculated as $0.3 \times 0.7 \times 0.3 \times ... \times 0.3 = 0.000037$.

Table 1: Example of quality state scenarios

Scenario	Component type												Probability
	L1	L2	P1	P2	P3	P4	P5	P6	P7	P8	P9	P10	
1	1	0	1	0	0	1	1	1	0	1	0	1	0.000037
2	1	1	1	0	1	0	0	0	1	1	0	1	0.000037
3	0	1	1	1	1	1	1	0	1	1	0	0	0.000016
4	0	1	1	0	1	0	0	0	0	0	1	0	0.000467
5	1	1	1	0	1	1	1	0	1	1	1	1	0.000002

3.3. Two-stage stochastic programming formulation

Given the described scenario generation approach for random quality status, we can formulate our problem setting as a two-stage stochastic program with recourse. In a general two-stage stochastic programming model, the first stage decisions are taken when the decision maker does not have enough information about the outcome of uncertain parameters, while, the second stage decisions are implemented after the uncertainty is realized. In other words, the "second stage" decision is made when the complete information with respect to uncertain parameter(s) is available.

Referring to Figure 1, in our problem setting, in the first stage, the location of collection, disassembly, remanufacturing, bulk recycling, material recycling, and disposal facilities in the reverse network should be determined before the complete information on the quality status of returns is available. Thus, the binary location decisions are first stage decisions. Moreover, since the demand is deterministic, the uncertainty in quality status of returns does not affect the decisions on the quantity of brand-new durable products shipped form manufacturing facilities to end-users via distribution centers. Therefore, such forward flow decisions are also among the first stage decisions. Likewise, as the quantity of returns is deterministic, the reverse flow from end-users to collection sites and the flow from collection centers to disassembly facilities are also first stage decisions. Lastly, regardless of the quality state of returns, they contain precious raw materials that can also be recycled in material recycling centers. Accordingly, the flow of recyclable materials from disassembly centers to material recycling sites is considered as a first stage decision variable. Once the returns are graded in disassembly centers, a complete information on the number of recoverable modules and parts in addition to the mass of residues are available to decision maker. Consequently, the remaining flows in the reverse channel are referred to as the second stage decisions (recourse actions). The physical flows from various suppliers to manufacturing centers are also considered as second stage decisions due to the impact of uncertain quality states on them. The notations used in the mathematical model is listed in Appendix A. The two-stage stochastic programming formulation with fixed recourse can be stated as follows.

$$\begin{aligned}
\text{Maximize} \quad & \sum_{j\in J}\sum_{k\in K} Pk_k X^2_{jk} - \sum_{i\in I}\sum_{j\in J} ci_i X^1_{ij} - \sum_{i\in I}\sum_{j\in J} tj_{ij} X^1_{ij} - \sum_{j\in J}\sum_{k\in K} cj_j X^2_{jk} \\
& - \sum_{j\in J}\sum_{k\in K} tk_{jk} X^2_{jk} - \sum_{k\in K}\sum_{c\in C} cc_c X^3_{kc} - \sum_{k\in K}\sum_{c\in C} tc_{kc} X^3_{kc} \\
& - \sum_{c\in C}\sum_{a\in A} ca_a X^4_{ca} - \sum_{c\in C}\sum_{a\in A} ta_{ca} X^4_{ca} - \sum_{c\in C}\sum_{a\in A} Pr X^4_{ca} \\
& - \sum_{a\in A}\sum_{g\in G}\sum_{r\in R} cg_{gr} X^5_{agr} - \sum_{a\in A}\sum_{g\in G}\sum_{r\in R} tg_{agr} X^5_{agr} - \sum_{c\in C} fc_c Y^1_c \\
& - \sum_{a\in A} fa_a Y^2_a - \sum_{m\in M} fm_m Y^3_m - \sum_{b\in B} fb_b Y^4_b - \sum_{g\in G} fg_g Y^5_g - \sum_{d\in D} fd_d Y^6_d \\
& + \sum_{s\in S} \pi_s Q(Y^1_c, Y^2_a, Y^3_m, Y^4_b, Y^5_g, Y^6_d, X^1_{ij}, X^2_{jk}, X^3_{kc}, X^4_{ca}, X^5_{agr}, \boldsymbol{\xi}_s)
\end{aligned} \tag{1}$$

$$\text{subject to} \quad \sum_{i\in I} X^1_{ij} = \sum_{k\in K} X^2_{jk} \quad \forall\, j \in J \tag{2}$$

$$\sum_{j\in J} X^2_{jk} = dk_k \quad \forall\, k \in K \tag{3}$$

$$\sum_{c\in C} X^3_{kc} = \psi dk_k \quad \forall\, k \in K \tag{4}$$

$$\sum_{k\in K} X^3_{kc} \geq \sum_{a\in A} X^4_{ca} \quad \forall\, c \in C \tag{5}$$

$$\sum_{c\in C}\sum_{a\in A} X^4_{ca} \geq \lambda \sum_{k\in K}\sum_{c\in C} X^3_{kc} \tag{6}$$

$$\sum_{c\in C} \alpha_r X^4_{ca} = \sum_{g\in G} X^5_{agr} \quad \forall\, a \in A, \forall\, r \in R \tag{7}$$

$$\sum_{j\in J} X^1_{ij} \leq cai_i \quad \forall\, i \in I \tag{8}$$

$$\sum_{i\in I} X^1_{ij} \leq caj_j \quad \forall\, j \in J \tag{9}$$

$$\sum_{k \in K} X^3_{kc} \leq cac_c YC_c \quad \forall\, c \in C \tag{10}$$

$$\sum_{c \in C} X^4_{ca} \leq caa_a YA_a \quad \forall\, a \in A \tag{11}$$

where $Q(Y^1_c, Y^2_a, Y^3_m, Y^4_b, Y^5_g, Y^6_d, X^1_{ij}, X^2_{jk}, X^3_{kc}, X^4_{ca}, X^5_{agr}, \boldsymbol{\xi}_s)$ is the optimal value of the following problem:

$$\begin{aligned}
\text{Maximize} \quad & \sum_{m \in M}\sum_{w \in W}\sum_{l \in L} Pw_l QW_{mwls} + \sum_{a \in A}\sum_{o \in O}\sum_{p \in P} Ps_p QS_{aops} \\
& + \sum_{g \in G}\sum_{e \in E}\sum_{r \in R} Pe_r QE_{gers} - \sum_{z \in Z}\sum_{i \in I}\sum_{p \in P} cz_{zp} QI_{zips} \\
& - \sum_{u \in U}\sum_{i \in I}\sum_{r \in R} cu_{ur} NI_{uirs} - \sum_{h \in H}\sum_{i \in I}\sum_{l \in L} cx_{hl} XI_{hils} \\
& - \sum_{b \in B}\sum_{g \in G}\sum_{r \in R} cg_{gr} NG_{bgrs} - \sum_{a \in A}\sum_{m \in M}\sum_{l \in L} cm_{ml} QM_{amls} \\
& - \sum_{a \in A}\sum_{b \in B} cb_b QB_{abs} - \sum_{b \in B}\sum_{d \in D} cd_d ND_{bds} \\
& - \sum_{g \in G}\sum_{d \in D}\sum_{r \in R} cd_d XD_{gdrs} - \sum_{b \in B} crBR_{bs} \\
& - \sum_{z \in Z}\sum_{i \in I}\sum_{p \in P} ti_{zip} QI_{zips} - \sum_{u \in U}\sum_{i \in I}\sum_{r \in R} ri_{uir} NI_{uirs} \\
& - \sum_{h \in H}\sum_{i \in I}\sum_{l \in L} si_{hil} XI_{hils} - \sum_{a \in A}\sum_{m \in M}\sum_{l \in L} tm_{aml} QM_{amls} \\
& - \sum_{a \in A}\sum_{b \in B} tb_{ab} QB_{abs} - \sum_{b \in B}\sum_{g \in G}\sum_{r \in R} rg_{bgr} NG_{bgrs} \\
& - \sum_{g \in G}\sum_{d \in D}\sum_{r \in R}\sum_{s \in S} sd_{gd} XD_{gdrs} - \sum_{b \in B}\sum_{d \in D} rd_{bd} ND_{bds} \\
& - \sum_{a \in A}\sum_{o \in O}\sum_{p \in P} ts_{aop} QS_{aops} - \sum_{m \in M}\sum_{w \in W}\sum_{l \in L} tw_{mwl} QW_{mwls} \\
& - \sum_{g \in G}\sum_{e \in E}\sum_{r \in R} te_{ger} QE_{gers} - \sum_{a \in A}\sum_{i \in I}\sum_{p \in P} tz_{aip} QZ_{aips}
\end{aligned}$$

$$- \sum_{m \in M} \sum_{i \in I} \sum_{l \in L} tx_{mil} QX_{mils} - \sum_{g \in G} \sum_{i \in I} \sum_{r \in R} tu_{gir} QU_{girs} \tag{12}$$

subject to

$$\sum_{z \in Z} QI_{zips} + \sum_{a \in A} QZ_{aips} = \phi_p \sum_{j \in J} X^1_{ij} \quad \forall\, i \in I, \forall\, p \in P \tag{13}$$

$$\sum_{u \in U} NI_{uirs} + \sum_{g \in G} QU_{girs} = \mu_r \sum_{j \in J} X^1_{ij} \quad \forall\, i \in I, \forall\, r \in R \tag{14}$$

$$\sum_{h \in H} XI_{hils} + \sum_{m \in M} QX_{mils} = \omega_l \sum_{j \in J} X^1_{ij} \quad \forall\, i \in I, \forall\, l \in L \tag{15}$$

$$\sum_{c \in C} \gamma_{ps} X^4_{ca} = \sum_{i \in I} QZ_{aips} + \sum_{o \in O} QS_{aops} \quad \forall\, a \in A, \forall\, p \in P \tag{16}$$

$$\sum_{a \in A} QS_{aops} \leq ds_{op} \quad \forall\, o \in O, \forall\, p \in P \tag{17}$$

$$\sum_{c \in C} \beta_s X^4_{ca} = \sum_{b \in B} QB_{abs} \quad \forall\, a \in A \tag{18}$$

$$\sum_{c \in C} \delta_{ls} X^4_{ca} = \sum_{m \in M} QM_{amls} \quad \forall\, a \in A, \forall\, l \in L \tag{19}$$

$$\sum_{a \in A} QM_{amls} = \sum_{w \in W} QW_{mwls}$$

$$+ \sum_{i \in I} QX_{mils} \quad \forall\, m \in M, \forall\, l \in L \tag{20}$$

$$\sum_{m \in M} QW_{mwls} \leq dw_{wl} \quad \forall\, w \in W, \forall\, l \in L \tag{21}$$

$$\sum_{a \in A} \eta_r QB_{abs} = \sum_{g \in G} NG_{bgrs} \quad \forall\, b \in B, \forall\, r \in R \tag{22}$$

$$\sum_{a \in A} QB_{abs} = \sum_{g \in G} \sum_{r \in R} NG_{bgrs} + \sum_{d \in D} ND_{bds}$$

$$+ BR_{bs} \quad \forall\, b \in B \tag{23}$$

$$\sum_{a \in A} \tau_r X^5_{agr} + \sum_{b \in B} \tau_r NG_{bgrs} = \sum_{d \in D} XD_{gdrs} \quad \forall\, g \in G, \forall\, r \in R \tag{24}$$

$$\sum_{g \in G} QE_{gers} \leq de_{er} \quad \forall\, e \in E, \forall\, r \in R \tag{25}$$

$$\sum_{a\in A} X^5_{agr} + \sum_{b\in B} NG_{bgrs} = \sum_{i\in I} QU_{girs} + \sum_{e\in E} QE_{gers}$$
$$+ \sum_{d\in D} XD_{gdrs} \quad \forall\, g \in G, \forall\, r \in R \tag{26}$$

$$\sum_{i\in I} QI_{zips} \leq caz_{zp} \quad \forall\, z \in Z, \forall\, p \in P \tag{27}$$

$$\sum_{i\in I} NI_{uirs} \leq cau_{ur} \quad \forall\, u \in U, \forall\, r \in R \tag{28}$$

$$\sum_{i\in I} XI_{hils} \leq cax_{hl} \quad \forall\, h \in H, \forall\, l \in L \tag{29}$$

$$\sum_{a\in A} QM_{amls} \leq cam_{ml} Y^3_m \quad \forall\, m \in M, \forall\, l \in L \tag{30}$$

$$\sum_{a\in A} QB_{abs} \leq cab_b Y^4_b \quad \forall\, b \in B \tag{31}$$

$$\sum_{a\in A} X^5_{agr} + \sum_{b\in B} NG_{bgrs} \leq cag_{gr} Y^5_g \quad \forall\, g \in G, \forall\, r \in R \tag{32}$$

$$\sum_{b\in B} ND_{bds} + \sum_{g\in G}\sum_{r\in R} XD_{gdrs} \leq cad_d Y^6_d \quad \forall\, d \in D \tag{33}$$

In the two-stage stochastic programming model (1)-(33), the objective function is to maximize the expected profit for all realized quality state scenarios. The objective function is composed of the revenue from selling brand-new products and recovered components and recycled materials in addition to the fixed costs of opening facilities as well as processing, procurement, and shipping costs in the CLSC network. Constraint (2)-(3) ensure flow balance at each distribution center and demand satisfaction at each end-user zone. Constraint (4) ensures that all the returned products are collected at the collection centers. Constraint (5) ensures that the total flow to the disassembly facilities, i.e., acquired returns, cannot exceed the total amount of returned products available in collection centers. Constraint (6) ensures that the OEM acquires a substantial portion of the return stream for recovery purposes. This constraint reflects the environmental concerns regarding the harmful effects of leaving used durable products in the environment. Constraint (7) ensures that the total flow outgoing from disassembly centers to all recycling centers is equal to the incoming flow to each disassembly center from all collection centers, multiplied by recyclable mass coefficient α_r. Constraints (8)-(11) are capacity restrictions. Constraints (13)-(15) ensure that the total outgoing flow from each manufacturing center is equal to the total incoming flow into this facility from suppliers and reverse channel. Constraints (16)-(19) ensure flow conservation at each disassembly center. Constraints (20)-(21) ensure the flow conservation at each remanufacturing facility. Constraints (22)-(23) ensure flow conservation at each bulk recycling center. Constraints (24)-(26) are flow conservation restrictions at each material recycling center. Constraints (27)-(33) impose capacity restrictions on supply chain facilities. Constraints (17), (21), and (25) represent partial demand satisfaction of recovered components and recycled raw materials at secondary markets.

The two-stage stochastic programming model (1)-(33) involves an extremely large number of recourse problems $Q(Y_c^1, Y_a^2, Y_m^3, Y_b^4, Y_g^5, Y_d^6, X_{ij}^1, X_{jk}^2, X_{kc}^3, X_{ca}^4, X_{agr}^5, \boldsymbol{\xi}_s)$. This leads to a computationally intractable model. Therefore, a scenario-based reduction approach would be required to alleviate the computational complexity of the proposed model.

4. Scenario reduction algorithm

In this section , we articulate a scenario reduction framework based on fast forward selection algorithm adapted to the particular structure of the uncertainty set for quality status of returns. The main idea behind the scenario reduction scheme is to preserve the most pertinent scenarios through eliminating the doubtful scenarios to occur. Consequently, it determines the best approximation of the current set of scenarios with respect to a probability distance measure, i.e., most often Monge-Kantorovich distance.

We let Ω be the probability distribution carried by n-dimensional scenarios $s_i = (\xi_{s_i}^{l_1}, \xi_{s_i}^{l_2}, ..., \xi_{s_i}^{l_L}, \xi_{s_i}^{p_1}, \xi_{s_i}^{p_2}, ..., \xi_{s_i}^{p_P})$ in which l and p indicate, respectively, index of modules and parts. For instance, l_1 denotes the first type of modules while p_3 represents the third type of parts in the reverse BOM. Each scenario s_i is associated with probability π_i for $i = \{1, ..., |S|\}$ such that $\sum_{i=1}^{|S|} \pi_i = 1$. Further, we let $\overline{\Omega}$ be the set of reduced probability distribution, compared to Ω, carried by finitely scenarios $s_j = (\xi_{s_j}^{l_1}, \xi_{s_j}^{l_2}, ..., \xi_{s_j}^{l_L}, \xi_{s_j}^{p_1}, \xi_{s_j}^{p_2}, ..., \xi_{s_j}^{p_P})$ with probability $\overline{\pi_j}$ for $j \in \{1, ..., |S|\} \setminus J$, where J denotes the index set of eliminated scenarios. The minimal Monge-Kantorovich distance between Ω and $\overline{\Omega}$ is then attained as follows (Theorem 2.1. in [8]).

$$D(\Omega, \overline{\Omega}) = \sum_{i \in J} \pi_i . \min_{j \notin J} c(s_i, s_j) \tag{34}$$

and the probability of the preserved scenario s_j of $\overline{\Omega}$, $j \notin J$, is given by the so-called *redistribution rule*:

$$\overline{\pi_j} = \pi_j + \sum_{i \in J_j} \pi_i \tag{35}$$

where $c(s_i, s_j)$ is a distance metric between scenarios s_i and s_j and $J_j = \{i \in J : j = j(i)\}$ and $j(i) \in \arg\min_{j \notin J} c(s_i, s_j); \forall i \in J$. The interpretation of the redistribution rule, equation (35), is that the modified value of the probability of a preserved scenario is equal to sum of its initial probability and all probabilities of eliminated scenarios that are closest to it concerning the distance metric c.

The reduction problem (34) states that the initial scenario set involving 2^n number of scenarios is covered by two sets $J \subset \{1, ..., |S|\}$ and $\{1, ..., |S|\} \backslash J$ such that the cover has the minimum value, i.e., $D(\Omega, \overline{\Omega})$. This problem is therefore a set covering problem, which is NP-hard. In [8], an efficient heuristic algorithm based on Monge-Kantorovich distance has been developed to determine the optimal scenario set reduction. The concept of fast forward selection algorithm is the recursive selection of scenarios that will not be eliminated. The first scenario to be preserved is the one that has the minimum sum of the distances to the unselected scenarios. In the subsequent steps, the distance of the unselected scenarios is updated by comparing these scenarios to the selected set. Thus, the sum of the distances of the unselected scenarios is calculated and the next scenario to be preserved is selected akin to the first scenario in the selected set. This process terminates once a specified number (m) of scenarios has been selected to be preserved. In the end, the probabilities of each non-selected scenario is added to its closest selected scenario concerning the redistribution rule (35).

The first step of forward selection algorithm involves constructing the distance matrix. Euclidean distance has been a common metric used in stochastic optimization literature. In this study, the distance norm is adapted to the particular structure of the uncertainty set. More specifically, we differentiate between modules and parts in the reverse BOM of a durable product. The rationale behind that is the different characteristics and economic values residing in these components. Hence, from the practical standpoint, the modified distance matrix better reflects the heterogeneity residing in each quality state scenario compared to a classical distance matrix. To this end, the following modified Euclidean norm is considered as a distance measure between every pair of scenarios s_i and s_j.

$$
\begin{aligned}
c(s_i, s_j) &= ||\xi^{\boldsymbol{l}}_{s_i} - \xi^{\boldsymbol{l}}_{s_j}||_2 + ||\xi^{\boldsymbol{p}}_{s_i} - \xi^{\boldsymbol{p}}_{s_j}||_2 \\
&= \sqrt{(\xi^{l_1}_{s_i} - \xi^{l_1}_{s_j})^2 + ... + (\xi^{l_L}_{s_i} - \xi^{l_L}_{s_j})^2} + \sqrt{(\xi^{p_1}_{s_i} - \xi^{p_1}_{s_j})^2 + ... + (\xi^{p_P}_{s_i} - \xi^{p_P}_{s_j})^2}
\end{aligned}
$$

The fast forward selection algorithm is outlined in Algorithm 1. This algorithm starts with an empty selected set of scenarios and iteratively updates it by adding the scenario minimizing Monge-Kantorovich distance between original and selected sets. In the first step, the distance matrix corresponding to the original set of scenarios is constructed using the modified Euclidean distance metric described above. Then, the minimum distance is computed (line 2 in the algorithm description) and immediately the first scenario to be preserved is identified. Consequently, the set of selected scenarios is updated. In the following steps, the distance matrix is updated concerning the fourth line and distances between scenarios in the original and selected sets is calculated (line 5). The scenario with the minimum distance value is selected as the next scenario not to be eliminated and the selected set is updated. The probability of the scenarios in the selected set is computed through the redistribution rule (35).

Algorithm 1 - Fast forward selection

1: **Step 1:** $c_{ij}^{[1]} := c(s_i, s_j) \quad \forall i, j \in \{1, ..., |S|\}; i \neq j$

2: $z_j^{[1]} := \sum_{\substack{i=1 \\ i \neq j}}^{|S|} \pi_i c_{ij}^{[1]} \quad \forall j \in \{1, ..., |S|\}$

3: $j_1 \in \arg\min_{j \in \{1,...,|S|\}} z_j^{[1]}, J^{[1]} := \{1, ..., |S|\} \backslash \{j_1\}$

4: **Step k:** $c_{ij}^{[k]} := \min\{c_{ij}^{[k-1]}, c_{ij_{k-1}}^{[k-1]}\} \quad \forall i, j \in J^{[k-1]}; i \neq j$

5: $z_j^{[k]} := \sum_{i \in J^{[k-1]} \backslash \{j\}} \pi_i c_{ij}^{[k]} \quad \forall j \in J^{[k-1]}$

6: $j_k \in \arg\min_{j \in J^{[k-1]}} z_j^{[k]}, J^{[k]} := J^{[k-1]} \backslash \{j_k\}$

7: **Step $m+1$:** Applying the redistribution rule (35)

5. Solution methodology

The mixed-integer programming model (1)-(33) is a large-scale optimization problem. It is due to several types of binary decision variables corresponding to location of facilities in the reverse network, the generic reverse BOM of the returned durable product, and the large yet tractable number of reduced recourse problems. This model can be tackled by an efficient solution approach which we devise based on L-shaped algorithm. In classical L-shaped method, the deterministic equivalent (original) problem is decomposed into a master problem (MP) and a set of recourse subproblems (RSP) associated with each random scenario defined in the original model. The MP comprises the first stage variables, an artificial variable, and a set of first stage constraints. This problem is the reformulation of the original model which is solved by a cutting plane algorithm such that, at each iteration, whenever a feasible solution to the original problem is found, an optimality cut associated with the set of scenarios are added to the MP. Otherwise, a number of feasibility cuts corresponding to infeasible scenarios are added. The solution to the MP and the expected value of the solutions to the recourse problems gives, respectively, upper and lower bounds to the original problem. The solution process terminates once an optimal solution is found or a prescribed optimality gap is satisfied.

In what follows, we first provide the classical L-shaped reformulation, then we propose algorithmic enhancements in order to speed-up its convergence rate.

5.1. L-shaped reformulation

In L-shaped scheme, all the second stage flow variables are projected out and the master problem includes the first stage facility locations and flow variables along with a surrogate variable. We let $\overline{\boldsymbol{X}}$ and $\overline{\boldsymbol{Y}}$ denote a tentative first stage solution. The corresponding RSP for each scenario s can be stated as follows.

$$\text{Maximize} \quad Q(\overline{\boldsymbol{X}}, \overline{\boldsymbol{Y}}, \boldsymbol{\xi}_s) \tag{36}$$

$$\text{subject to} \quad (17), (20) - (23), (25), (27) - (29)$$

$$\sum_{z \in Z} QI_{zips} + \sum_{a \in A} QZ_{aips} = \phi_p \sum_{j \in J} \overline{X_{ij}^1} \quad \forall\, i \in I, \forall\, p \in P \tag{37}$$

$$\sum_{u \in U} NI_{uirs} + \sum_{g \in G} QU_{girs} = \mu_r \sum_{j \in J} \overline{X_{ij}^1} \quad \forall\, i \in I, \forall\, r \in R \tag{38}$$

$$\sum_{h \in H} XI_{hils} + \sum_{m \in M} QX_{mils} = \omega_l \sum_{j \in J} \overline{X_{ij}^1} \quad \forall\, i \in I, \forall\, l \in L \tag{39}$$

$$\sum_{c \in C} \gamma_{ps} \overline{X_{ca}^4} = \sum_{i \in I} QZ_{aips} + \sum_{o \in O} QS_{aops} \quad \forall\, a \in A, \forall\, p \in P \tag{40}$$

$$\sum_{c \in C} \beta_s \overline{X_{ca}^4} = \sum_{b \in B} QB_{abs} \quad \forall\, a \in A \tag{41}$$

$$\sum_{c\in C}\delta_{ls}\overline{X^4_{ca}} = \sum_{m\in M} QM_{amls} \quad \forall\, a\in A, \forall\, l\in L \tag{42}$$

$$\sum_{b\in B}\tau_r NG_{bgrs} - \sum_{d\in D} XD_{gdrs} = -\sum_{a\in A}\tau_r\overline{X^5_{agr}} \quad \forall\, g\in G, \forall\, r\in R \tag{43}$$

$$\sum_{a\in A}\overline{X^5_{agr}} = \sum_{i\in I} QU_{girs} + \sum_{e\in E} QE_{gers} + \sum_{d\in D} XD_{gdrs}$$

$$-\sum_{b\in B} NG_{bgrs} \quad \forall\, g\in G, \forall\, r\in R \tag{44}$$

$$\sum_{a\in A} QM_{amls} \le cam_{ml}\overline{Y^3_m} \quad \forall\, m\in M, \forall\, l\in L \tag{45}$$

$$\sum_{a\in A} QB_{abs} \le cab_b\overline{Y^4_b} \quad \forall\, b\in B \tag{46}$$

$$\sum_{b\in B} NG_{bgrs} \le cag_{gr}\overline{Y^5_g} - \sum_{a\in A}\overline{X^5_{agr}} \quad \forall\, g\in G, \forall\, r\in R \tag{47}$$

$$\sum_{b\in B} ND_{bds} + \sum_{g\in G}\sum_{r\in R} XD_{gdrs} \le cad_d\overline{Y^6_d} \quad \forall\, d\in D \tag{48}$$

To formulate the dual of the recourse subproblem, we define $\boldsymbol{\upsilon^1}$,..., $\boldsymbol{\upsilon^{21}}$, in which $\upsilon^5_{ops}, \upsilon^9_{wls}, \upsilon^{13}_{ers}, \upsilon^{15}_{zps}, \upsilon^{16}_{urs}, \upsilon^{17}_{hls}, \upsilon^{18}_{mls}, \upsilon^{19}_{bs}, \upsilon^{20}_{grs}, \upsilon^{21}_{ds} \in \mathbb{R}^+$, as the set of dual variable vectors corresponding to the constraints of RSP. The dual problem for each scenario s, namely DRSP, can then be formulated as follows.

$$\begin{aligned}
\text{Minimize} \quad Z_{\boldsymbol{\upsilon}}(\overline{\boldsymbol{X}}, \overline{\boldsymbol{Y}}, \boldsymbol{\xi}_s) = {} & \sum_{i\in I}\sum_{j\in J}\overline{X^1_{ij}}\Big(\sum_{p\in P}\phi_p\upsilon^1_{ips} + \sum_{r\in R}\mu_r\upsilon^2_{irs} + \sum_{l\in L}\omega_l\upsilon^3_{ils}\Big) \\
& + \sum_{a\in A}\sum_{c\in C}\overline{X^4_{ca}}\Big(\sum_{p\in P}\gamma_{ps}\upsilon^4_{aps} + \beta_s\upsilon^6_{as} + \sum_{l\in L}\delta_l\upsilon^7_{als}\Big) + \sum_{o\in O}\sum_{p\in P} ds_{op}\upsilon^5_{ops} \\
& + \sum_{w\in W}\sum_{l\in L} dw_{wl}\upsilon^9_{wls} + \sum_{g\in G}\sum_{a\in A}\overline{X^5_{agr}}\Big(\sum_{r\in R}\upsilon^{12}_{grs} + \sum_{r\in R}\upsilon^{14}_{grs}\Big) \\
& + \sum_{e\in E}\sum_{r\in R} de_{er}\upsilon^{13}_{ers} + \sum_{z\in Z}\sum_{p\in P} caz_{zp}\upsilon^{15}_{zps} + \sum_{u\in U}\sum_{r\in R} cau_{ur}\upsilon^{16}_{urs}
\end{aligned}$$

$$+\sum_{h\in H}\sum_{l\in L} cax_{hl}\upsilon^{17}_{hls} + \sum_{m\in M}\sum_{l\in L} cam_{ml}\overline{Y^3_m}\upsilon^{18}_{mls} + \sum_{b\in B} cab_b\overline{Y^4_b}\upsilon^{19}_{bs}$$

$$+\sum_{g\in G}\sum_{r\in R}\left(cag_{gr}\overline{Y^5_g} - \sum_{a\in A}\overline{X^5_{agr}}\right)\upsilon^{20}_{grs} + \sum_{d\in D} cad_d\overline{Y^6_d}\upsilon^{21}_{ds} \tag{49}$$

$$\text{subject to} \quad (\boldsymbol{\upsilon^1}, \boldsymbol{\upsilon^2}, ..., \boldsymbol{\upsilon^{21}}) \in \Delta_s \tag{50}$$

where Δ_s is the polyhedron defined by the constraints of the DRSP. We let $\rho_s(\boldsymbol{.})$ denote the first stage variables free terms in the objective function of the DRSP and we introduce a surrogate variable θ representing an upper bound on the expected recourse function $\mathbb{E}_{\boldsymbol{\xi}}[Q(\boldsymbol{X}, \boldsymbol{Y}, \boldsymbol{\xi})]$. Thus, we can reformulate the master problem of the two-stage stochastic programming model (1)-(33) as follows.

$$\begin{aligned}
\text{Maximize} \quad & \theta + \sum_{j\in J}\sum_{k\in K} Pk_k X^2_{jk} - \sum_{i\in I}\sum_{j\in J} ci_i X^1_{ij} - \sum_{i\in I}\sum_{j\in J} tj_{ij} X^1_{ij} \\
& - \sum_{j\in J}\sum_{k\in K} cj_j X^2_{jk} - \sum_{j\in J}\sum_{k\in K} tk_{jk} X^2_{jk} - \sum_{k\in K}\sum_{c\in C} cc_c X^3_{kc} \\
& - \sum_{k\in K}\sum_{c\in C} tc_{kc} X^3_{kc} - \sum_{c\in C}\sum_{a\in A} ca_a X^4_{ca} - \sum_{c\in C}\sum_{a\in A} ta_{ca} X^4_{ca} \\
& - \sum_{c\in C}\sum_{a\in A} Pr X^4_{ca} - \sum_{a\in A}\sum_{g\in G}\sum_{r\in R} cg_{gr} X^5_{agr} - \sum_{a\in A}\sum_{g\in G}\sum_{r\in R} tg_{agr} X^5_{agr} \\
& - \sum_{c\in C} fc_c Y^1_c - \sum_{a\in A} fa_a Y^2_a - \sum_{m\in M} fm_m Y^3_m - \sum_{b\in B} fb_b Y^4_b \\
& - \sum_{g\in G} fg_g Y^5_g - \sum_{d\in D} fd_d Y^6_d
\end{aligned} \tag{51}$$

subject to $\quad (2) - (11)$

$$\theta \le \sum_{s\in S}\pi_s\left(\rho_s(\boldsymbol{\hat{\upsilon}^{n^T}}) + \sum_{i\in I}\sum_{j\in J} X^1_{ij}\left(\sum_{p\in P}\phi_p\hat{\upsilon}^1_{ips} + \sum_{r\in R}\mu_r\hat{\upsilon}^2_{irs} + \sum_{l\in L}\omega_l\hat{\upsilon}^3_{ils}\right)\right.$$

$$
\begin{aligned}
&+\sum_{a\in A}\sum_{c\in C}X^4_{ca}\bigg(\sum_{p\in P}\gamma_{ps}\hat{\upsilon}^4_{aps}+\beta_s\hat{\upsilon}^6_{as}+\sum_{l\in L}\delta_l\hat{\upsilon}^7_{als}\bigg)\\
&+\sum_{g\in G}\sum_{a\in A}X^5_{agr}\bigg(\sum_{r\in R}\hat{\upsilon}^{12}_{grs}+\sum_{r\in R}\hat{\upsilon}^{14}_{grs}\bigg)+\sum_{m\in M}\sum_{l\in L}cam_{ml}Y^3_m\hat{\upsilon}^{18}_{mls}\\
&+\sum_{b\in B}cab_bY^4_b\hat{\upsilon}^{19}_{bs}+\sum_{g\in G}\sum_{r\in R}\bigg(cag_{gr}Y^5_g-\sum_{a\in A}X^5_{agr}\bigg)\hat{\upsilon}^{20}_{grs}+\sum_{d\in D}cad_dY^6_d\hat{\upsilon}^{21}_{ds}\bigg)
\end{aligned}
\tag{52}
$$

$$
\begin{aligned}
&0\le\rho_{s'}(\hat{\boldsymbol{\kappa}}^{\boldsymbol{n}^T})+\sum_{i\in I}\sum_{j\in J}X^1_{ij}\bigg(\sum_{p\in P}\phi_p\hat{\kappa}^1_{ips'}+\sum_{r\in R}\mu_r\hat{\kappa}^2_{irs'}+\sum_{l\in L}\omega_l\hat{\kappa}^3_{ils'}\bigg)\\
&+\sum_{a\in A}\sum_{c\in C}X^4_{ca}\bigg(\sum_{p\in P}\gamma_{ps}\hat{\kappa}^4_{aps'}+\beta_s\hat{\kappa}^6_{as'}+\sum_{l\in L}\delta_l\hat{\kappa}^7_{als'}\bigg)\\
&+\sum_{g\in G}\sum_{a\in A}X^5_{agr}\bigg(\sum_{r\in R}\hat{\kappa}^{12}_{grs'}+\sum_{r\in R}\hat{\kappa}^{14}_{grs'}\bigg)+\sum_{m\in M}\sum_{l\in L}cam_{ml}Y^3_m\hat{\kappa}^{18}_{mls'}\\
&+\sum_{b\in B}cab_bY^4_b\hat{\kappa}^{19}_{bs'}+\sum_{g\in G}\sum_{r\in R}\bigg(cag_{gr}Y^5_g-\sum_{a\in A}X^5_{agr}\bigg)\hat{\kappa}^{20}_{grs'}\\
&+\sum_{d\in D}cad_dY^6_d\hat{\kappa}^{21}_{ds'}\quad\forall s'\in S
\end{aligned}
\tag{53}
$$

$$
\boldsymbol{X}\in\mathbb{R}^+,\boldsymbol{Y}\in\{0,1\}\tag{54}
$$

where $\boldsymbol{\kappa}$ indicates extreme rays of Δ whenever the DRSP is unbounded for a given first stage solution in scenario s'. As shown above, the set of optimality cuts for each scenario s has been aggregated to produce the single optimality cut (52), while (53) represents the feasibility cut for each infeasible scenario s'.

We also let F and C be the cost vectors in the objective function of the first stage problem. The classical L-shaped method is outlined in Algorithm 2. Pilot computational tests have shown a poor convergence rate of the classical L-shaped method. To circumvent this issue, we proceed with proposing two different enhancement strategies in the next section.

Algorithm 2 - Classical L-shaped method

$UB \leftarrow \infty$, $LB \leftarrow -\infty$

while $(UB - LB)/UB \leq \epsilon$ **do**

Solve the MP

$UB \leftarrow \bar{\theta} + F^T\overline{\boldsymbol{Y}} + C^T\overline{\boldsymbol{X}}$

Solve the DRSP for each scenario s

if the DRSP is unbounded **then**

  Add the corresponding feasibility cut (53) to the MP

else

  Generate the corresponding optimality cut

end if

if The DRSP was optimal for all realiztion of scenarios **then**

  Add the aggregated optimality cut (52) to the MP

  $LB \leftarrow \max\,(LB, \sum_s \pi_s Z_{\boldsymbol{v}}(\overline{\boldsymbol{X}}, \overline{\boldsymbol{Y}}, \boldsymbol{\xi}_s) + F^T\overline{\boldsymbol{Y}} + C^T\overline{\boldsymbol{X}})$

end if

end while

5.2. Algorithmic refinements

5.2.1. Induced constraints

We note that various types of valid inequalities (induced constraints) can be added to the MP. In the early iterations of L-shaped algorithm, because the iterative algorithm is initialized from empty subsets of extreme rays and extreme points, the solution to the MP might be infeasible for the original model, which leads to the generation of the feasibility cuts. Induced constraints restrict the feasible region of the MP and transfer more information on RSPs to the MP. Hence, they dramatically diminish the number of feasibility cuts throughout the solution process and enhance the convergence of L-shaped method by helping the MP to identify close to optimal solutions. Given the structure of model (1)-(33), the following constraints can be added to the MP as induced constraints.

$$\sum_{c \in C} cac_c Y_c^1 \geq \sum_{k \in K} \psi dk_k \tag{55}$$

$$\sum_{a \in A} caa_a Y_a^2 \geq \lambda\psi \sum_{k \in K} dk_k \tag{56}$$

$$\sum_{m \in M} cam_{ml} Y_m^3 \geq \delta_{ls} \lambda\psi \sum_{k \in K} dk_k \quad \forall\, l \in L, \forall\, s \in S \tag{57}$$

$$\sum_{b \in B} cab_b Y_b^4 \geq \beta_s \lambda\psi \sum_{k \in K} dk_k \quad \forall\, s \in S \tag{58}$$

$$\sum_{g \in G} cag_{gr} Y_g^5 \geq \alpha_r \lambda\psi \sum_{k \in K} dk_k \quad \forall\, r \in R \tag{59}$$

$$\sum_{d \in D} Y_d^6 \geq 1 \tag{60}$$

The set of inequalities (55)-(59) ensures installing enough capacity in the reverse channel. Constraint (60) ensures that at least one disposal center is installed in the reverse network.

5.2.2. Pareto-optimal cuts

A smart idea to enhance the convergence of the L-shaped algorithm is to strengthen the deepness of the optimality cuts. In some applications, multiple optimal solutions might exist to the DRSP, each providing a potentially different cut. To choose the deepest cut among various optimality cuts corresponding to the multiple optimal solutions, Magnanti and Wong [26] proposed a cut selection scheme, which improves the convergence of the

Benders decomposition algorithm. In the context of our problem of interest, the definition of a stronger cut can be expressed as follows according to Magnanti and Wong.

Definition 1. Given that $\boldsymbol{X}$ and $\boldsymbol{Y}$ represent, respectively, the set of first stage continuous and binary decision variables in model (1)-(33), the optimality cut generated from the dual solution vectors $(\boldsymbol{\upsilon_1^1}, ..., \boldsymbol{\upsilon_1^7}, \boldsymbol{\upsilon_1^9}, \boldsymbol{\upsilon_1^{12}}, ..., \boldsymbol{\upsilon_1^{21}}) \in \Delta_s$ dominates the cut generated from $(\boldsymbol{\upsilon_2^1}, ..., \boldsymbol{\upsilon_2^7}, \boldsymbol{\upsilon_2^9}, \boldsymbol{\upsilon_2^{12}}, ..., \boldsymbol{\upsilon_2^{21}}) \in \Delta_s$ if and only if

$$
\begin{aligned}
&\sum_{s \in S} \pi_s \Bigg(\rho_s(\hat{\boldsymbol{\upsilon}}_{\boldsymbol{1}}^{\boldsymbol{n}^T}) + \sum_{i \in I} \sum_{j \in J} X_{ij}^1 \Big(\sum_{p \in P} \phi_p \hat{\upsilon}_{1ips}^1 + \sum_{r \in R} \mu_r \hat{\upsilon}_{1irs}^2 + \sum_{l \in L} \omega_l \hat{\upsilon}_{1ils}^3 \Big) \\
&+ \sum_{a \in A} \sum_{c \in C} X_{ca}^4 \Big(\sum_{p \in P} \gamma_{ps} \hat{\upsilon}_{1aps}^4 + \beta_s \hat{\upsilon}_{1as}^6 + \sum_{l \in L} \delta_l \hat{\upsilon}_{1als}^7 \Big) \\
&+ \sum_{g \in G} \sum_{a \in A} X_{1agr}^5 \Big(\sum_{r \in R} \hat{\upsilon}_{1grs}^{12} + \sum_{r \in R} \hat{\upsilon}_{1grs}^{14} \Big) + \sum_{m \in M} \sum_{l \in L} cam_{ml} Y_m^3 \hat{\upsilon}_{1mls}^{18} \\
&+ \sum_{b \in B} cab_b Y_b^4 \hat{\upsilon}_{1bs}^{19} + \sum_{g \in G} \sum_{r \in R} \Big(cag_{gr} Y_g^5 - \sum_{a \in A} X_{agr}^5 \Big) \hat{\upsilon}_{1grs}^{20} + \sum_{d \in D} cad_d Y_d^6 \hat{\upsilon}_{1ds}^{21} \Bigg) \\
&\leq \sum_{s \in S} \pi_s \Bigg(\rho_s(\hat{\boldsymbol{\upsilon}}_{\boldsymbol{2}}^{\boldsymbol{n}^T}) + \sum_{i \in I} \sum_{j \in J} X_{ij}^1 \Big(\sum_{p \in P} \phi_p \hat{\upsilon}_{2ips}^1 + \sum_{r \in R} \mu_r \hat{\upsilon}_{2irs}^2 + \sum_{l \in L} \omega_l \hat{\upsilon}_{2ils}^3 \Big) \\
&+ \sum_{a \in A} \sum_{c \in C} X_{ca}^4 \Big(\sum_{p \in P} \gamma_{ps} \hat{\upsilon}_{2aps}^4 + \beta_s \hat{\upsilon}_{2as}^6 + \sum_{l \in L} \delta_l \hat{\upsilon}_{2als}^7 \Big) \\
&+ \sum_{g \in G} \sum_{a \in A} X_{agr}^5 \Big(\sum_{r \in R} \hat{\upsilon}_{2grs}^{12} + \sum_{r \in R} \hat{\upsilon}_{2grs}^{14} \Big) + \sum_{m \in M} \sum_{l \in L} cam_{ml} Y_m^3 \hat{\upsilon}_{2mls}^{18} \\
&+ \sum_{b \in B} cab_b Y_b^4 \hat{\upsilon}_{2bs}^{19} + \sum_{g \in G} \sum_{r \in R} \Big(cag_{gr} Y_g^5 - \sum_{a \in A} X_{agr}^5 \Big) \hat{\upsilon}_{2grs}^{20} + \sum_{d \in D} cad_d Y_d^6 \hat{\upsilon}_{2ds}^{21} \Bigg)
\end{aligned}
$$

for all $\boldsymbol{X}$ and $\boldsymbol{Y}$ with strict inequality for at least one extreme point. A Pareto-optimal cut is not dominated by any other cut. Now, let Λ be a polyhedron stated as $\Lambda = \{(\boldsymbol{X}, \boldsymbol{Y}) : (2) - (11)\text{are satisifed}\}$.

Definition 2. Core point: any point $(\boldsymbol{X^0}, \boldsymbol{Y^0})$ contained in the relative interior of the convex hull of Λ is said to be a core point, i.e, $(\boldsymbol{X^0}, \boldsymbol{Y^0}) \in ri(\Lambda^c)$, in which $ri(.)$ and Λ^c, respectively, denote the relative interior and the convex hull of Λ.

Given the above definitions, the Pareto-cut selection scheme based on [26] for the CLSC network design problem under investigation is presented in Appendix B. In this study, we adapt the Pareto-optimal cut generation approach presented in Papadakos [27], an enhancement to Magnanti and Wong's method. In [27], it has been shown that the normalization constraint (see constraint B.2 in Appendix B) can be disregarded through varying the value of the core point at each iteration of the solution process. In this approach, once the solution to the MP yields feasible RSPs, the value of the core point can be updated through the convex combination of the MP solution and the previous value of the core point. In this regard the auxiliary dual recourse subproblem (auxiliary-DRSP) can be stated as follows.

$$
\begin{aligned}
\text{Minimize} \quad Z_{\boldsymbol{\upsilon}}(\boldsymbol{X^0}, \boldsymbol{Y^0}, \boldsymbol{\xi}_s) = & \sum_{i \in I} \sum_{j \in J} X_{ij}^{1^0} \left(\sum_{p \in P} \phi_p \upsilon_{ips}^1 + \sum_{r \in R} \mu_r \upsilon_{irs}^2 + \sum_{l \in L} \omega_l \upsilon_{ils}^3 \right) \\
& + \sum_{a \in A} \sum_{c \in C} X_{ca}^{4^0} \left(\sum_{p \in P} \gamma_{ps} \upsilon_{aps}^4 + \beta_s \upsilon_{as}^6 + \sum_{l \in L} \delta_l \upsilon_{als}^7 \right) + \sum_{o \in O} \sum_{p \in P} ds_{op} \upsilon_{ops}^5 \\
& + \sum_{w \in W} \sum_{l \in L} dw_{wl} \upsilon_{wls}^9 + \sum_{g \in G} \sum_{a \in A} X_{agr}^{5^0} \left(\sum_{r \in R} \upsilon_{grs}^{12} + \sum_{r \in R} \upsilon_{grs}^{14} \right) \\
& + \sum_{e \in E} \sum_{r \in R} de_{er} \upsilon_{ers}^{13} + \sum_{z \in Z} \sum_{p \in P} caz_{zp} \upsilon_{zps}^{15} + \sum_{u \in U} \sum_{r \in R} cau_{ur} \upsilon_{urs}^{16} \\
& + \sum_{h \in H} \sum_{l \in L} cax_{hl} \upsilon_{hls}^{17} + \sum_{m \in M} \sum_{l \in L} cam_{ml} Y_m^{3^0} \upsilon_{mls}^{18} + \sum_{b \in B} cab_b Y_b^{4^0} \upsilon_{bs}^{19} \\
& + \sum_{g \in G} \sum_{r \in R} \left(cag_{gr} Y_g^{5^0} - \sum_{a \in A} X_{agr}^{5^0} \right) \upsilon_{grs}^{20} + \sum_{d \in D} cad_d Y_d^{6^0} \upsilon_{ds}^{21}
\end{aligned}
$$

$$\text{subject to} \quad (\boldsymbol{v^1}, \boldsymbol{v^2}, ..., \boldsymbol{v^{21}}) \in \Delta_s \tag{61}$$

The optimal solution to auxiliary-DRSP (61) is used to generate the Pareto-optimal cut. We note that finding a core point in Λ^c is a difficult act since the description of the convex hull is unknown a priori. Therefore, rather than using a core point in Λ^c, we choose the core point in the linear programming relaxation of Λ to generate the Pareto-optimal cut. This cut is a non-dominated cut on Λ^{LP} though it might be dominated in Λ^c. We let non-negative parameter λ^c indicate the weight of the core point ($\boldsymbol{X^0}$, $\boldsymbol{Y^0}$) in the convex combination that updates the value of the core point throughout the solution process. Empirically, it has been shown that 0.5 most often yields the best results ([27]). An outline of the proposed enhanced L-shaped method is presented in Algorithm 3.

6. Numerical results

In this section, we illustrate some numerical experiments to provide an analysis of the CLSC network design problem under investigation. To this end, first, we present a typical large household appliance example, i.e., washing machine [28], as a suitable case of durable products and provide a description of randomly generated data sets based on the CLSC/RSC design literature ([21], [29]), which ensures varying values of input parameters. Then, we proceed with a detailed representation of the performance of the proposed solution method on two reduced sets of scenarios with different sizes, i.e., 500 and 1000. Finally, using the enhanced L-shaped method for each scenario set, we evaluate the performance of the scenario reduction algorithm.

Algorithm 3 - Enhanced L-shaped method

$UB \leftarrow \infty$, $LB \leftarrow -\infty$, $\lambda^c \leftarrow 0.5$
Add induced constraints (55)-(60) to the MP
Start with an initial core point $(\boldsymbol{X}^{\mathbf{0}}, \boldsymbol{Y}^{\mathbf{0}})$
while $(UB - LB)/UB \leq \epsilon$ **do**
Solve auxiliary-DRSP (61) for each scenario s
Add the aggregated Pareto-optimal cut (52) to the MP
Solve the MP
$UB \leftarrow \bar{\theta} + F^T\overline{\boldsymbol{Y}} + C^T\overline{\boldsymbol{X}}$
Solve the DRSP for each scenario s
if the DRSP is unbounded **then**
    Add the corresponding feasibility cut (53) to the MP
    Update core point only one time $(\boldsymbol{X}^{\mathbf{0}}, \boldsymbol{Y}^{\mathbf{0}}) \leftarrow \lambda^c \boldsymbol{(X^{0}, Y^{0})} + \zeta$
else
    Generate the corresponding optimality cut
end if
if The DRSP was optimal for all realiztion of scenarios **then**
    Add the aggregated optimality cut (52) to the MP
    $LB \leftarrow \max\,(LB, \sum_s \pi_s Z_{\boldsymbol{v}}(\overline{\boldsymbol{X}}, \overline{\boldsymbol{Y}}, \boldsymbol{\xi}_s) + F^T\overline{\boldsymbol{Y}} + C^T\overline{\boldsymbol{X}})$
    $(\boldsymbol{X}^{\mathbf{0}}, \boldsymbol{Y}^{\mathbf{0}}) \leftarrow \lambda^c \boldsymbol{(X^{0}, Y^{0})} + (1-\lambda^c)(\overline{\boldsymbol{X}}, \overline{\boldsymbol{Y}})$
end if
end while

The fast forward selection algorithm and the accelerated L-shaped method are implemented in C++ programming language. More particularly, the proposed decomposition algorithm is implemented in C++ using Concert Technology with IBM-ILOG CPLEX 12.60. We also employ the default settings of CPLEX and conduct all the experiments on an Intel Quad Core 3.40 GHz with 8 GB RAM.

6.1. Computational experiments

We consider the recovery network of a used washing machine which consists of various components as given in Table 2. Recalling the scenario generation approach introduced in Section 3.2 and the number of components of the washing machine in our experiments, i.e., twelve components, the grading process yields 2^{12} or 4096 quality state scenarios which is relatively large. The parameter settings of the proposed mathematical formulation is presented in Appendix C. Further, capacities of facilities are randomly generated following a reasonable relationship with the reverse BOM, demands parameters, and return ratio. Demands of recycled raw materials at the corresponding secondary marketplaces are also randomly generated considering the reverse BOM and the return ratio. Shipping costs are selected from $Uniform(4,\ 7)$ for the washing machine, $Uniform(1,\ 4)$ for each type of components, and $Uniform(0.1,\ 0.5)$ for raw materials, bulk of residues, and wastes.

We also apply fast forward selection algorithm described in earlier section where two reduced scenario sets of sizes 500 and 1000 are selected out of the set of 4096 scenarios. Then, we employ five classes of problems, each with

Table 2: The washing machine parts and modules

Description	Value
ϕ_p	washing tube:1, cover:1, balance:1, frame:1, hose:1, condenser:1, small electric parts:1, electric wire:1, transformer:1, PCB board:1
ω_l	motor:1, clutch:1

5 randomly generated test instances, for both sets of scenarios as shown in Table 3. We also show detailed information on the size of problem classes in Table 4.

6.2. Computational results

To assess the computational efficiency of the proposed enhanced L-shaped method, we define an optimality gap $\epsilon\%$ in addition to a time limit as the stopping criteria for this algorithm. More precisely, the solution process terminates once either the optimality gap falls below 0.5% or the solution time exceeds 3600 seconds. As for the core point $(\boldsymbol{X^0}, \boldsymbol{Y^0})$, point $\boldsymbol{Y^0}$ is fixed to 0.5 for all the first stage binary variables at the beginning of the solution approach. Moreover, to pick a suitable value for point $\boldsymbol{X^0}$, after fixing the value of $\boldsymbol{Y^0}$ to 0.5, the resulting subproblem (1)-(11) is solved considering a small

Table 3: Problem classes

Class	$\|Z\|$	$\|U\|$	$\|H\|$	$\|I\|$	$\|J\|$	$\|K\|$	$\|C\|$	$\|A\|$	$\|M\|$	$\|B\|$	$\|G\|$	$\|D\|$	$\|O\|$	$\|W\|$	$\|E\|$	$\|S\|$
C1	10	3	2	5	10	60	10	10	10	10	10	5	30	30	30	500
																1000
C2	10	3	2	5	10	80	10	10	10	10	10	5	40	40	40	500
																1000
C3	10	3	2	5	15	100	15	15	15	15	15	7	50	50	50	500
																1000
C4	10	3	2	5	15	120	15	15	15	15	15	7	60	60	60	500
																1000
C5	10	3	2	5	20	140	20	20	20	20	20	10	70	70	70	500
																1000

Table 4: Size of the deterministic equivalent problems

Class	$\|S\|$	Constraints	Continuous Vars.	Binary Vars.
C1	500	476706	3261650	55
	1000	953206	6521650	55
C2	500	551746	4012050	55
	1000	1103246	8022050	55
C3	500	705326	7276475	82
	1000	1410326	14548975	55
C4	500	780366	8402075	82
	1000	1560366	16799575	82
C5	500	934446	13022300	110
	1000	1868446	26037300	110

positive value as the lower bound for $\boldsymbol{X^0}$ to ensure generating an interior point. We also solve all 50 test instances with CPLEX in a maximum time limit of 7200 seconds and within the stopping gap tolerance of 0.5% to avoid tail-off effect. It should be noted that the numerical results of the classical L-shaped method are not reported in this section due to the poor convergence rate of this algorithm on pilot tests. Tables 5 and 6 present, respectively, computational results for the reduced sets of 500 and 1000 scenarios. These tables also show computational statistics of CPLEX including CPU time in seconds followed by the value of the objective function reported by CPLEX within the dedicated time limit. The last column entitled by "Gap" represents an average on the relative difference between the profit values reported by the enhanced L-shaped method and CPLEX for each class of problems within their corresponding time limits.

Table 5: Computational results on problem classes for $|S| = 500$

Class	Enhanced L-shaped			CPLEX		
	Runtime (sec)	Iterations	Profit	Runtime (sec)	Profit	Gap
C1	320	22	23,583,400	$\geq$ 7200	23,523,900	3.33%
	170	12	26,655,700	$\geq$ 7200	22,921,100	
	280	19	25,156,500	$\geq$ 7200	24,860,600	
	269	19	24,681,000	$\geq$ 7200	24,383,200	
	244	17	26,100,800	$\geq$ 7200	26,093,900	
C2	443	27	35,837,400	$\geq$ 7200	35,211,400	17.07%
	527	32	34,890,800	$\geq$ 7200	34,688,000	
	224	14	36,404,200	$\geq$ 7200	35,984,800	
	278	17	34,448,900	$\geq$ 7200	31,359,400	
	523	31	37,958,400	$\geq$ 7200	10,287,600	
C3	969	32	44,375,400	$\geq$ 7200	4,181,020	88.29%
	521	17	40,886,900	$\geq$ 7200	6,483,960	
	1119	36	45,205,700	$\geq$ 7200	6,253,750	
	704	24	42,834,000	$\geq$ 7200	3,127,920	
	531	18	43,602,900	$\geq$ 7200	5,294,590	
C4	1382	36	51,663,200	$\geq$ 7200	10,866,000	73.02%
	1154	31	56,215,500	$\geq$ 7200	15,416,000	
	763	21	58,737,500	$\geq$ 7200	19,074,500	
	764	21	54,991,600	$\geq$ 7200	No solution	
	823	23	55,213,400	$\geq$ 7200	No solution	
C5	2835	38	65,911,400	$\geq$ 7200	12,020,400	86.90%
	2900	41	60,880,800	$\geq$ 7200	No solution	
	2348	31	63,561,500	$\geq$ 7200	No solution	
	2680	33	58,883,900	$\geq$ 7200	4,692,950	
	2530	36	62,967,200	$\geq$ 7200	No solution	

Table 6: Computational results on problem classes for $|S| = 1000$

Class	Enhanced L-shaped			CPLEX		
	Runtime (sec)	Iterations	Profit	Runtime (sec)	Profit	Gap
C1	598	21	23,722,300	$\geq$ 7200	1,615,900	39.10%
	331	12	26,802,200	$\geq$ 7200	24,555,100	
	580	19	25,299,200	$\geq$ 7200	24,626,900	
	556	18	24,823,600	$\geq$ 7200	24,342,000	
	455	16	26,242,400	$\geq$ 7200	2,792,950	
C2	857	26	36,006,600	$\geq$ 7200	31,597,900	49.43%
	900	27	35,106,500	$\geq$ 7200	17,316,500	
	460	14	36,585,700	$\geq$ 7200	14,543,600	
	580	17	34,634,300	$\geq$ 7200	12,017,300	
	1324	39	38,117,700	$\geq$ 7200	15,757,200	
C3	1848	30	44,619,300	$\geq$ 7200	No solution	-
	1154	19	41,121,600	$\geq$ 7200	No solution	
	1720	28	45,440,300	$\geq$ 7200	No solution	
	1438	24	43,077,100	$\geq$ 7200	No solution	
	970	16	43,835,900	$\geq$ 7200	No solution	
C4	1944	26	51,663,200	$\geq$ 7200	No solution	-
	2472	33	56,215,500	$\geq$ 7200	No solution	
	1663	22	58,737,500	$\geq$ 7200	No solution	
	1768	23	54,991,600	$\geq$ 7200	No solution	
	1588	22	55,213,400	$\geq$ 7200	No solution	
C5	$\geq$ 3600	26	66,258,600	$\geq$ 7200	M	-
	$\geq$ 3600	27	65,256,200	$\geq$ 7200	M	
	$\geq$ 3600	25	63,761,100	$\geq$ 7200	M	
	$\geq$ 3600	25	59,212,300	$\geq$ 7200	M	
	$\geq$ 3600	27	63,307,000	$\geq$ 7200	M	

M: out-of-memory

As far as the results reported in Table 5 concerned, the proposed L-shaped method solves all 25 test instances of different sizes to optimality in a reasonable amount of time while CPLEX is only able to find a feasible solution for most of test problems. In particular, the feasible solutions identified by CPLEX for C3 to C5 are considerably far from the optimal solutions given by the L-shaped method observing the huge average gap between the values of the objective function reported by two approaches as indicated in the last column. Note that, in the last two classes of problems, CPLEX cannot find any feasible solution to five test instances within two hours, denoted by "No solution". Accordingly, the gap values presented in the last column are associated with solvable test instances by both approaches. This can be explained by the fact that the deterministic equivalent problem which CPLEX attempts to solve involves a large number of recourse problems associated with the representative quality state scenarios. Hence, model (1)-(33), even with reduced number of scenarios, is itself a very difficult to solve problem for the commercial software. This observation supports the call for an efficient solution approach. As opposed to CPLEX, the proposed enhanced L-shaped algorithm can easily handle realistic size problems such that the average runtime in classes one to four is 600 seconds, which verifies the advantage of the refinement strategies. Note that, in the case of the largest test problems (class C5), we observe, on average, a 77.42% solution time increase compared to the other four classes. Nonetheless, all test instances are solvable in the alloted time by the proposed decomposition scheme.

Likewise, Table 6 reports the same statistics in the case of 1000 scenarios. Analysis of this table leads to similar implications as in the case of 500 scenarios. However, concerning the size of the set of scenarios, i.e., 1000, there exist a few exceptions that need to be clarified. Firstly, the runtime for the accelerated L-shaped method increases 12.77% on average over all test instances excluding the fifth class. Secondly, the test instances of the last class cannot be solved within one hour until the dedicated optimality gap, i.e., $\epsilon = 0.5\%$, is reached by the solution algorithm. However, for this class of problems, the relative difference between the lower and upper bounds of the solution process after an hour is quite tight (0.54% on average over test instances of C5), which is not far from the stopping optimality gap of 0.5%. Finally, when the computational results of CPLEX are considered, we observe an out-of-memory state in the last class along with its failure to generate a feasible solution within two hours of runtime in test instances of the third and fourth classes. The above discussion demonstrates the effectiveness of the proposed accelerated L-shaped algorithm for solving our problem of interest.

6.3. Analysis of fast forward selection algorithm

Herein, we evaluate the performance of fast forward selection algorithm through comparing the numerical results of the reduced scenario sets presented in the previous section. To this end, we compare the values of the expected profit obtained by considering reduced sets of scenarios with the one that we estimate through considering all possible scenarios for the random quality status of the return stream. Let us indicate the optimal solution of model (1)-(33) by V_{2SP}, which is obtained by considering a reduced set of scenarios. Now, the first stage variables in (1)-(33) are substituted with the corresponding optimal values obtained by applying the proposed L-shaped algorithm for the reduced two-stage stochastic program. Then, the resulting recourse subproblems are solved for all 4096 quality state scenarios. The expected value of the profit function is therefore calculated over all scenarios and denoted by EV_{2SP}. The relative difference (RD) measure, representing the gap between EV_{2SP} and V_{2SP}, can be stated as follows.

$$RD = 100 \times |(V_{2SP} - EV_{2SP})|/V_{2SP}$$

It should be noted that the RD measure indicates how good the reduced scenario set, obtained by the proposed fast forward selection algorithm, represents the whole set of scenarios. The steps described above are repeated for each test instance of our experiments. Table 7 summarizes the average value of RD over all five test instances for each class of problems, in cases of 500 and 1000 scenarios.

Table 7: The average value of RD for $|S| = 500$

# Scenarios	C1	C2	C3	C4	C5
500	1.25%	1.17%	1.21%	1.14%	1.19%
1000	0.69%	0.65%	0.67%	0.71%	0.70%

As can be seen Table 7, the RD values are quite insignificant, i.e., less than 2%. It means that both reduced sets of 500 and 1000 scenarios provide good quality solutions to our stochastic problem. This observation verifies the capability of fast forward selection algorithm in finding reduced sets of scenarios, that are reliable representations of 4096 quality state scenarios.

Moreover, analyzing these results, it can be inferred that the larger reduced scenario set, i.e., 1000 scenarios, provides a better approximation to the true stochastic CLSC network design problem involving a large number of scenarios. However, it should be remembered that, in the case of 1000 scenarios, the average CPU time increases by 12.77% over solvable test instances against that of 500 scenarios. From the above discussion, it can be understood that if the decision maker prefers to obtain more accurate solutions to model (1)-(33), he/she should pay the cost of computational time. The proposed solution framework along with the scenario reduction method allows the decision maker to have a perfect insight on possible trade-offs between computational time and the accuracy of solutions, and therefore to select a solution that is consistent with his/her willingness to invest computational efforts to design the CLSC network.

7. Conclusion

In this paper, we introduced a CLSC network design problem under uncertain quality status of the return stream, which is applicable to the case of durable products. The underlying uncertainty is considered as the availability of each component in the reverse BOM and modeled as discrete scenarios with Bernoulli probability distribution. Accordingly, we proposed a two-stage mixed-integer stochastic program to explicitly address uncertainty in this problem. In order to tackle the intractable number of scenarios resulting from several components that exist in the reverse BOM of a typical durable product, we adapted fast forward selection algorithm to our problem of interest to preserve the most pertinent binary scenarios in the deterministic equivalent problem. Moreover, we developed a solution method based on L-shaped algorithm, further enhanced with additional acceleration strategies, including several valid inequalities and non-dominated optimality cuts. Our computational experiments demonstrated an outstanding capability of the proposed algorithm for the CLSC network design problem.

We believe that our numerical results are general in nature and remain valid in the context of any durable product. The proposed solution framework together with the employed scenario reduction technique can be used to solve realistic-sized problems. More specifically, the computational experiments performed show that the average solution time are 1012 and 1962 seconds, receptively, for cases of 500 and 1000 scenarios. Furthermore, our findings indicate that the adapted fast forward selection algorithm is potent enough to construct a subset of the complete scenario set that leads to good quality solutions.

This research can be extended in several directions. Given a planning horizon discretized by a set of finite time periods, the proposed model can be extended to a dynamic CLSC network design problem in which the uncertainty in quantity of returns and demands can be addressed along with uncertain quality status of cores. Another avenue of research is to deal with the uncertain quality state through the robust optimization approach. This might alleviate the computational complexity of the stochastic programming method.

Acknowledgment

The authors are grateful for the financial supports provided by Le Fonds de recherche du Québec-Nature et technologies (FRQNT) and the Natural Sciences and Engineering Research Council of Canada (NSERC).

References

[1] V. D. R. Guide Jr, L. N. Van Wassenhove, OR FORUM-the evolution of closed-loop supply chain research, Operations research 57 (1) (2009) 10–18.

[2] M. Fleischmann, H. R. Krikke, R. Dekker, S. D. P. Flapper, A characterisation of logistics networks for product recovery, Omega 28 (6) (2000) 653–666.

[3] N. Aras, D. Aksen, A. Gönül Tanuğur, Locating collection centers for incentive-dependent returns under a pick-up policy with capacitated vehicles, European Journal of Operational Research 191 (3) (2008) 1223–1240.

[4] N. Aras, D. Aksen, Locating collection centers for distance-and incentive-dependent returns, International Journal of Production Economics 111 (2) (2008) 316–333.

[5] K. Das, A. H. Chowdhury, Designing a reverse logistics network for optimal collection, recovery and quality-based product-mix planning, International Journal of Production Economics 135 (1) (2012) 209–221.

[6] W. Chen, B. Kucukyazici, V. Verter, M. J. Sáenz, Supply chain design for unlocking the value of remanufacturing under uncertainty, European Journal of Operational Research 247 (3) (2015) 804–819.

[7] J. R. Birge, F. Louveaux, Introduction to stochastic programming, Springer Science & Business Media, 2011.

[8] H. Heitsch, W. Römisch, Scenario reduction algorithms in stochastic programming, Computational optimization and applications 24 (2-3) (2003) 187–206.

[9] J. Dupačová, N. Gröwe-Kuska, W. Römisch, Scenario reduction in stochastic programming, Mathematical programming 95 (3) (2003) 493–511.

[10] R. M. Van Slyke, R. Wets, L-shaped linear programs with applications to optimal control and stochastic programming, SIAM Journal on Applied Mathematics 17 (4) (1969) 638–663.

[11] J. F. Benders, Partitioning procedures for solving mixed-variables programming problems, Numerische Mathematik 4 (1) (1962) 238–252.

[12] V. Jayaraman, V. Guide Jr, R. Srivastava, A closed-loop logistics model for remanufacturing, Journal of the Operational Research Society 50 (5) (1999) 497–508.

[13] M. Fleischmann, P. Beullens, J. M. Bloemhof-Ruwaard, L. N. Wassenhove, The impact of product recovery on logistics network design, Production and Operations Management 10 (2) (2001) 156–173.

[14] H. Krikke, J. Bloemhof-Ruwaard, L. Van Wassenhove, Concurrent product and closed-loop supply chain design with an application to refrigerators, International journal of production research 41 (16) (2003) 3689–3719.

[15] H. Üster, G. Easwaran, E. Akçali, S. Cetinkaya, Benders decomposition with alternative multiple cuts for a multi-product closed-loop supply chain network design model, Naval Research Logistics (NRL) 54 (8) (2007) 890–907.

[16] H. Min, H.-J. Ko, The dynamic design of a reverse logistics network from the perspective of third-party logistics service providers, International Journal of Production Economics 113 (1) (2008) 176–192.

[17] M. Jeihoonian, M. K. Zanjani, M. Gendreau, Accelerating Benders Decomposition for Closed-Loop Supply Chain Network Design: Case of Used Durable Products with Different Quality Levels, Technical Report CIRRELT-2014-58, Interuniversity Research Center on Enterprise Networks, Logistics and Transportation (CIRRELT) (2014) .

[18] E. Akçalı, S. Çetinkaya, H. Üster, Network design for reverse and closed-loop supply chains: An annotated bibliography of models and solution approaches, Networks 53 (3) (2009) 231–248.

[19] N. Aras, T. Boyaci, V. Verter, Designing the reverse logistics network. In: Ferguson, M., Souza, G. (Eds.), Closed-Loop Supply Chains: New Developments to Improve the Sustainability of Business Practices. CRC Press (2010) 67–97.

[20] M. I. G. Salema, A. P. Barbosa-Povoa, A. Q. Novais, An optimization model for the design of a capacitated multi-product reverse logistics network with uncertainty, European Journal of Operational Research 179 (3) (2007) 1063–1077.

[21] O. Listeş, A generic stochastic model for supply-and-return network design, Computers & Operations Research 34 (2) (2007) 417–442.

[22] M. S. Pishvaee, F. Jolai, J. Razmi, A stochastic optimization model for integrated forward/reverse logistics network design, Journal of Manufacturing Systems 28 (4) (2009) 107–114.

[23] M. C. Fonseca, Á. García-Sánchez, M. Ortega-Mier, F. Saldanha-da Gama, A stochastic bi-objective location model for strategic reverse logistics, Top 18 (1) (2010) 158–184.

[24] S. R. Cardoso, A. P. F. Barbosa-Póvoa, S. Relvas, Design and planning of supply chains with integration of reverse logistics activities under demand uncertainty, European Journal of Operational Research 226 (3) (2013) 436–451.

[25] L. J. Zeballos, C. A. Méndez, A. P. Barbosa-Povoa, A. Q. Novais, Multi-period design and planning of closed-loop supply chains with uncertain supply and demand, Computers & Chemical Engineering 66 (2014) 151–164.

[26] T. L. Magnanti, R. T. Wong, Accelerating Benders decomposition: Algorithmic enhancement and model selection criteria, Operations Research 29 (3) (1981) 464–484.

[27] N. Papadakos, Practical enhancements to the Magnanti–Wong method, Operations Research Letters 36 (4) (2008) 444–449.

[28] P.-J. Park, K. Tahara, I.-T. Jeong, K.-M. Lee, Comparison of four methods for integrating environmental and economic aspects in the end-of-life stage of a washing machine, Resources, conservation and recycling 48 (1) (2006) 71–85.

[29] S. A. Alumur, S. Nickel, F. Saldanha-da Gama, V. Verter, Multi-period reverse logistics network design, European Journal of Operational Research 220 (1) (2012) 67–78.

Appendix A.

Nomenclature

Sets

A	Set of disassembly centers
B	Set of bulk recycling centers
C	Set of collection centers
D	Set of disposal centers
E	Set of secondary markets for recycled materials
G	Set of material recycling centers
H	Set of module suppliers
I	Set of manufacturing centers
J	Set of distribution centers
K	Set of end-user zones
L	Set of modules
M	Set of remanufacturing centers
O	Set of secondary markets for spare parts
P	Set of parts
R	Set of raw materials
S	Set of quality state scenarios
U	Set of raw material suppliers
W	Set of secondary markets for modules

Z Set of part suppliers

Parameters

α_r The mass of recyclable material r in the returned product shipped to material recycling centers from disassembly centers

β_s The mass of residues in the returned product in scenario s shipped to bulk recycling centers from disassembly centers

δ_{ls} The number of remanufacturable module l in the returned product in scenario s shipped to remanufacturing centers from disassembly centers

η_r The ratio of recyclable material r shipped to material recycling centers from bulk recycling centers

γ_{ps} The number of reusable part p in the returned product in scenario s shipped to secondary markets and manufacturing centers from disassembly centers

λ The legislative target for recovery of the return stream

μ_r The volume of material r in each unit of product

ω_l The number of module l in each unit of product

ϕ_p The number of part p in each unit of product

ψ The rate of return

τ_r The ratio of non-recyclable material r shipped to disposal centers from bulk and material recycling centers

ca_a Processing cost per unit of the returned product at disassembly center a

caa_a Capacity of disassembly center a

cab_b Capacity of bulk recycling center b

cac_c Capacity of collection center c

cad_d Capacity of disposal center d

cag_{gr} Capacity of material recycling center g for raw material r

cai_i Capacity of manufacturing center i

caj_j Capacity of distribution center j

cam_{ml} Capacity of remanufacturing center m for module l

cau_{ur} Capacity of raw material supplier u for raw material r

cax_{hl} Capacity of module supplier h for module l

caz_{zp} Capacity of part supplier z for part p

cb_b Processing cost per kg of residues at recycling center b

cc_c Processing cost per unit of the returned product at collection center c

cd_d Disposal cost at disposal center d

cg_{gr} Recycling cost per kg of material r at material recycling center g

ci_i Production cost per unit of product at manufacturing center i

cj_j Distribution cost per unit of product at distribution center j

cm_{ml} Remanufacturing cost per unit of module l at remanufacturing center m

cr Outsourcing cost to third-party provider

cu_{ur} Procurement cost per kg of material r supplied by raw material supplier u

cx_{hl} Procurement cost per unit of module l supplied by module supplier h

cz_{zp} Procurement cost per unit of part p supplied by part supplier z

de_{er} Demand for material r at recycled material market e

dk_k Demand for the new product at end-user zone k

ds_{op} Demand for part p at spare market o

dw_{wl} Demand for module l at secondary market w

fa_a Fixed cost of opening disassembly center a

fb_b Fixed cost of opening bulk recycling center b

fc_c Fixed cost of opening collection center c

fd_d Fixed cost of opening disposal center d

fg_g Fixed cost of opening material recycling center g

fm_m Fixed cost of opening remanufacturing center m

Pe_r Unit price of material r at recycled material markets

Pk_k Unit price of the new product at end-user zone k

Pr Unit acquisition price of the returned product

Ps_p Unit price of part p at spare parts markets

Pw_l Unit price of module l at secondary markets

rd_{bd} Shipping cost per kg of wastes from bulk recycling center b to disposal center d

rg_{bgr} Shipping cost per kg of recyclable material r from bulk recycling center b to material recycling center g

ri_{uir} Shipping cost per kg of material r from material supplier u to manufacturing center i

sd_{gd} Shipping cost per kg of wastes from material recycling center g to disposal center d

si_{hil} Shipping cost per unit of module l from module supplier h to manufacturing center i

ta_{ca} Shipping cost per unit of the returned product from collection center c to disassembly center a

tb_{ab} Shipping cost per kg of residues from disassembly center a to bulk recycling center b

tc_{kc} Shipping cost per unit of the returned product from end-user k to collection center c

te_{ger} Shipping cost per kg of recycled material r from recycling center g to recycled material market e

tg_{agr} Shipping cost per kg of recyclable material r from disassembly center a to material recycling center g

ti_{zip} Shipping cost per unit of part p from part supplier z to manufacturing center i

tj_{ij} Shipping cost per unit of the new product from manufacturing center i to distribution center j

tk_{jk} Shipping cost per unit of the new product from distribution center j to end-user k

tm_{aml} Shipping cost per unit of module l from disassembly center a to remanufacturing center m

ts_{aop} Shipping cost per unit of part p from disassembly center a to spare market o

tu_{gir} Shipping cost per kg of recycled material r from material recycling center g to manufacturing centers i

tw_{mwl} Shipping cost per unit of module l from remanufacturing center m to secondary market w

tx_{mil} Shipping cost per unit of module l from remanufacturing center m to manufacturing center i

tz_{aip} Shipping cost per unit of part p from disassembly center a to manufacturing center i

The first stage decision variables

X_{ij}^1 The quantity of products shipped from manufacturing center i to distribution center j

X_{jk}^2 The quantity of products shipped from distribution center j to end-user zone k

X_{kc}^3 The quantity of returns shipped from end-user zone k to collection center c

X_{ca}^4 The quantity of returns shipped from collection center c to disassembly center a

X_{agr}^5 The quantity of recyclable material r shipped from disassembly center a to material recycling center g

Y_c^1 A binary variable which is equal to one if collection center c is opened and zero otherwise

Y_a^2 A binary variable which is equal to one if disassembly center a is opened and zero otherwise

Y_m^3 A binary variable which is equal to one if remanufacturing center m is opened and zero otherwise

Y_b^4 A binary variable which is equal to one if bulk recycling center b is opened and zero otherwise

Y_g^5 A binary variable which is equal to one if material recycling center g is opened and zero otherwise

Y_d^6 A binary variable which is equal to one if disposal center d is opened and zero otherwise

The second stage decision variables

BR_{bs} The volume of residues outsourced from bulk recycling center b to a third-party provider in scenario s

ND_{bds} The quantity of residues shipped from bulk recycling center b to disposal center d in scenario s

NG_{bgrs} The quantity of recyclable material r shipped from bulk recycling center b to material recycling center g in scenario s

NI_{uirs} The quantity of raw material r shipped from raw material supplier u to manufacturing center i in scenario s

QB_{abs} The quantity of residues shipped from disassembly center a to bulk recycling center b in scenario s

QE_{gers} The quantity of recycled material r shipped from material recycling center g to recycled material market e in scenario s

QI_{zips} The number of part p shipped from part supplier z to manufacturing center i in scenario s

QM_{amls} The number of module l shipped from disassembly center a to remanufacturing center m in scenario s

QS_{aops} The number of part p shipped from disassembly center a to spare parts market o in scenario s

QU_{girs} The quantity of recycled material r shipped from material recycling center g to manufacturing center i in scenario s

QW_{mwls} The number of module l shipped from remanufacturing center m to secondary market w in scenario s

QX_{mils} The number of module l shipped from remanufacturing center m to manufacturing center i in scenario s

QZ_{aips} The number of part p shipped from disassembly center a to manufacturing center i in scenario s

XD_{gdsr} The quantity of raw material r shipped from material recycling center g to disposal center d in scenario s

XI_{hils} The number of module l shipped from module supplier h to manufacturing center i in scenario s

Appendix B.

Considering Magnanti and Wong's approach, throughout the L-shaped algorithm, when the solution to the MP yields feasible RSPs for all scenarios, the following auxiliary dual subproblem has to be solved for each representative scenario.

$$\begin{aligned}
\text{Minimize} \quad Z_{\boldsymbol{\upsilon}}(\boldsymbol{X^0}, \boldsymbol{Y^0}, \boldsymbol{\xi}_s) = & \sum_{i\in I}\sum_{j\in J} X_{ij}^{1^0}\left(\sum_{p\in P}\phi_p\upsilon_{ips}^1 + \sum_{r\in R}\mu_r\upsilon_{irs}^2 + \sum_{l\in L}\omega_l\upsilon_{ils}^3\right) \\
& + \sum_{a\in A}\sum_{c\in C} X_{ca}^{4^0}\left(\sum_{p\in P}\gamma_{ps}\upsilon_{aps}^4 + \beta_s\upsilon_{as}^6 + \sum_{l\in L}\delta_l\upsilon_{als}^7\right) + \sum_{o\in O}\sum_{p\in P} ds_{op}\upsilon_{ops}^5 \\
& + \sum_{w\in W}\sum_{l\in L} dw_{wl}\upsilon_{wls}^9 + \sum_{g\in G}\sum_{a\in A} X_{agr}^{5^0}\left(\sum_{r\in R}\upsilon_{grs}^{12} + \sum_{r\in R}\upsilon_{grs}^{14}\right) \\
& + \sum_{e\in E}\sum_{r\in R} de_{er}\upsilon_{ers}^{13} + \sum_{z\in Z}\sum_{p\in P} caz_{zp}\upsilon_{zps}^{15} + \sum_{u\in U}\sum_{r\in R} cau_{ur}\upsilon_{urs}^{16} \\
& + \sum_{h\in H}\sum_{l\in L} cax_{hl}\upsilon_{hls}^{17} + \sum_{m\in M}\sum_{l\in L} cam_{ml}Y_m^{3^0}\upsilon_{mls}^{18} + \sum_{b\in B} cab_b Y_b^{4^0}\upsilon_{bs}^{19}
\end{aligned}$$

$$+\sum_{g\in G}\sum_{r\in R}\Big(cag_{gr}Y_g^{5^0}-\sum_{a\in A}X_{agr}^{5^0}\Big)\upsilon_{grs}^{20}+\sum_{d\in D}cad_d Y_d^{6^0}\upsilon_{ds}^{21} \tag{B.1}$$

subject to

$$\sum_{i\in I}\sum_{j\in J}\overline{X_{ij}^1}\Big(\sum_{p\in P}\phi_p\upsilon_{ips}^1+\sum_{r\in R}\mu_r\upsilon_{irs}^2+\sum_{l\in L}\omega_l\upsilon_{ils}^3\Big)$$
$$+\sum_{a\in A}\sum_{c\in C}\overline{X_{ca}^4}\Big(\sum_{p\in P}\gamma_{ps}\upsilon_{aps}^4+\beta_s\upsilon_{as}^6+\sum_{l\in L}\delta_l\upsilon_{als}^7\Big)+\sum_{o\in O}\sum_{p\in P}ds_{op}\upsilon_{ops}^5$$
$$+\sum_{w\in W}\sum_{l\in L}dw_{wl}\upsilon_{wls}^9+\sum_{g\in G}\sum_{a\in A}\overline{X_{agr}^5}\Big(\sum_{r\in R}\upsilon_{grs}^{12}+\sum_{r\in R}\upsilon_{grs}^{14}\Big)$$
$$+\sum_{e\in E}\sum_{r\in R}de_{er}\upsilon_{ers}^{13}+\sum_{z\in Z}\sum_{p\in P}caz_{zp}\upsilon_{zps}^{15}+\sum_{u\in U}\sum_{r\in R}cau_{ur}\upsilon_{urs}^{16}$$
$$+\sum_{h\in H}\sum_{l\in L}cax_{hl}\upsilon_{hls}^{17}+\sum_{m\in M}\sum_{l\in L}cam_{ml}\overline{Y_m^3}\upsilon_{mls}^{18}+\sum_{b\in B}cab_b\overline{Y_b^4}\upsilon_{bs}^{19}$$
$$+\sum_{g\in G}\sum_{r\in R}\Big(cag_{gr}\overline{Y_g^5}-\sum_{a\in A}\overline{X_{agr}^5}\Big)\upsilon_{grs}^{20}+\sum_{d\in D}cad_d\overline{Y_d^6}\upsilon_{ds}^{21}=Z_{\boldsymbol{\upsilon}}^*(\overline{\boldsymbol{X}},\overline{\boldsymbol{Y}},\boldsymbol{\xi}_s) \tag{B.2}$$

$$(\boldsymbol{\upsilon^1},\boldsymbol{\upsilon^2},....,\boldsymbol{\upsilon^{21}})\in\Delta_s \tag{B.3}$$

where $Z_{\boldsymbol{\upsilon}}^*(\overline{\boldsymbol{X}},\overline{\boldsymbol{Y}},\boldsymbol{\xi}_s)$ denotes the optimal value of the DRSP for the concerned scenario. The numerically unstable normalization constraint (B.2) ensures that the optimal solution of (B.1)-(B.3) is selected from the set of alternative optimal solutions to the DRSP. The aggregated optimality cut (52) generated using the solution of (B.1)-(B.3) is a Pareto-optimal cut.

Appendix C.

Tables C.8 to C.11 summarize parameter settings of model (1)-(33).

Table C.8: Parameter settings for modules

Description	Value	
	Motor	Clutch
cx_{hl}	75	35
Pw_l	150	75

Table C.9: Parameter settings for raw materials

Description	Value		
	Plastic	Steel	Copper
μ_r	3 kg	2 kg	1 kg
α_r	1.5 kg	1 kg	0.5 kg
cu_{ur}	0.75	0.5	3
pe_r	1.5	1	6

Table C.10: Parameter settings for parts

Type of part	Value	
	cz_{zp}	Ps_p
Washing tube	20	40
Cover	5	10
Balance	25	50
Frame	5	10
Condenser	15	30
Transformer	15	30
Small electric	5	10
Hose	20	40
Electric wire	20	40
PCB board	35	70

Table C.11: The value of the parameters

Description	Value	Description	Value
ci_i	4	cj_j	1
cc_c	1	ca_a	2
cm_m	3	cb_b	2
cg_{gr}	2	cd_d	2
cr	2	Pr	200
η_r	0.3	τ_r	0.2
ψ	0.6	λ	0.7
dk_k	$\{600, 601, ..., 1200\}$	ds_{op}	$\{30, 31, ..., 100\}$
dw_{wl}	$\{30, 31, ..., 100\}$	Pk_k	Uniform(700, 1300)
fc_c	Uniform(400000, 600000)	fa_a	Uniform(400000, 600000)
fm_m	Uniform(700000, 900000)	fb_b	Uniform(400000, 600000)
fg_g	Uniform(400000, 600000)	fd_d	Uniform(200000, 400000)